

Electronic Supplementary Information for
Room-temperature spin valve effect in TiCr_2N_4 monolayer

Haoshen Ye,^{a,b} Lisha Liu,^a Dongmei Bai,^c G. P. Zhang,^d Juntao Zhang,^a and Jianli Wang^{*,a}

^a School of Materials and Physics, China University of Mining and Technology, Xuzhou 221116, China

^b School of Physics, Southeast University, Nanjing 211189, China

^c School of Mathematics, China University of Mining and Technology, Xuzhou 221116, China

^d Department of Physics, Indiana State University, Terre Haute, Indiana 47809, USA

* Corresponding author.

E-mail address: jlwang@cumt.edu.cn (Jianli Wang).

I. Curie temperature. The evolution of magnetization as the function of temperature is simulated via Monte Carlo simulation based on the Heisenberg type Hamiltonian. A supercell of $12 \times 12 \times 1$ containing 288 Cr atoms is used for the Monte Carlo simulation. Steps for both achieving thermal equilibrium and sampling by Metropolis algorithm are set to 10^5 steps. The Heisenberg type Hamiltonian of TiCr_2N_4 can be described as

$$H = -J_{ij} \sum_{ij} \hat{S}_i \cdot \hat{S}_j - A_i \sum_i (\hat{S}_i \cdot \hat{z}_i)^2$$

where, J is the exchange parameter between site i and j . A_i and \hat{z}_i is the single-ion anisotropy energy and the unit vector of easy magnetization axis of Cr atom, respectively. Five different magnetic structures (Fig. S1) are considered for calculating the exchange parameters.

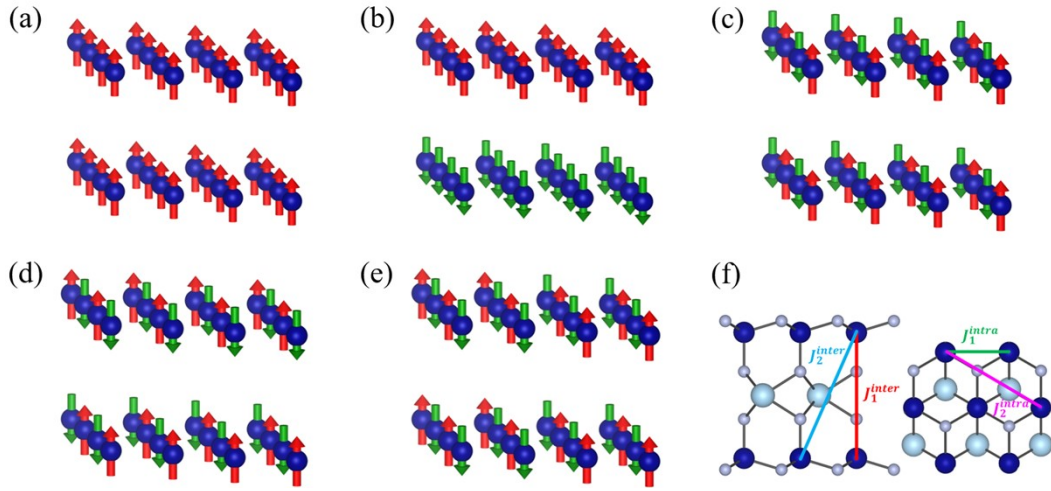


FIG. S1. Schematic of the five magnetic structures of monolayer TiCr_2N_4 . (a) FM, (b) inter-AFM, (c) intra-SAFM1, (d) intra-SAFM2, and (e) intra-ZAFM, respectively. (f) Schematic of the different exchange interactions.

The exchange parameters are obtained from magnetic energies calculations, which is written as

$$\begin{aligned} E_{FM} &= E_0 - 6J_1^{\text{intra}} - 6J_2^{\text{intra}} - J_1^{\text{inter}} - 6J_2^{\text{inter}} \\ E_{\text{inter-AFM}} &= E_0 - 6J_1^{\text{intra}} - 6J_2^{\text{intra}} + J_1^{\text{inter}} + 6J_2^{\text{inter}} \\ E_{\text{intra-SAFM1}} &= E_0 + 2J_1^{\text{intra}} + 2J_2^{\text{intra}} - J_1^{\text{inter}} + 2J_2^{\text{inter}} \\ E_{\text{intra-SAFM2}} &= E_0 + 2J_1^{\text{intra}} + 2J_2^{\text{intra}} + J_1^{\text{inter}} - 2J_2^{\text{inter}} \\ E_{\text{intra-ZAFM}} &= E_0 + 2J_1^{\text{intra}} - 2J_2^{\text{intra}} - J_1^{\text{inter}} + 2J_2^{\text{inter}} \end{aligned}$$

where, J^{intra} and J^{inter} correspond to exchange interactions between atoms from intralayer and interlayers, respectively. J_1 and J_2 correspond to the first- and second-nearest neighboring exchange interactions.

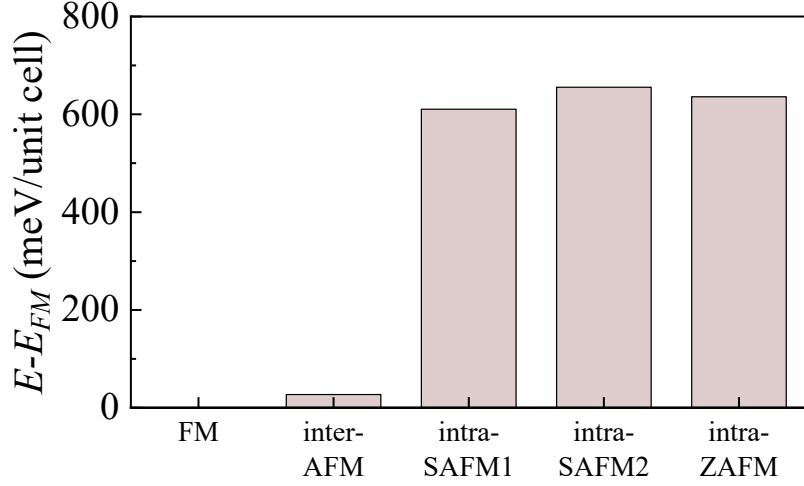


FIG. S2. The energy difference between the five magnetic structures and FM structure.

Table. S1. The calculated exchange parameters of TiCr_2N_4 monolayer.

	J_1^{intra}	J_2^{intra}	J_1^{inter}	J_2^{inter}
J (meV/Cr)	36.3	2.4	-6.8	2.3

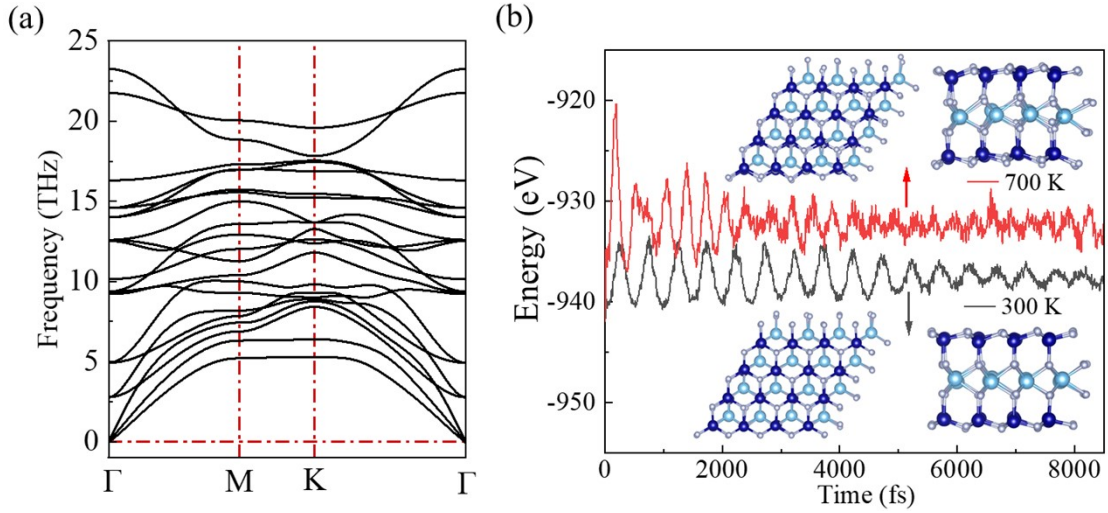


FIG. S3. (a) The phonon dispersion of TiCr_2N_4 monolayer. (b) The ab-initio molecular dynamic simulation of TiCr_2N_4 monolayer under 300 K and 700 K.

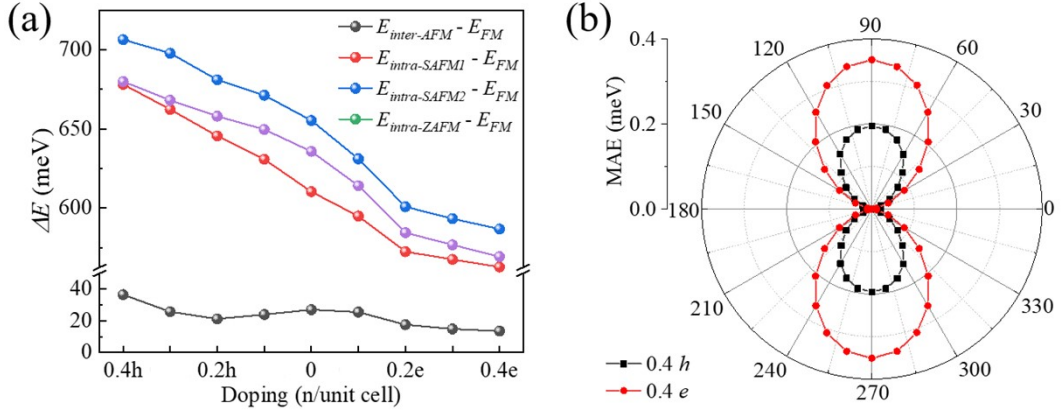


FIG. S4. (a) Energy difference between the FM structure and the four AFM structures under electrostatic doping. (b) MAE of TiCr_2N_4 monolayer under 0.4 electron and hole doping per unit cell. The 0° and 90° correspond to the in-plane and out-of-plane directions, respectively.

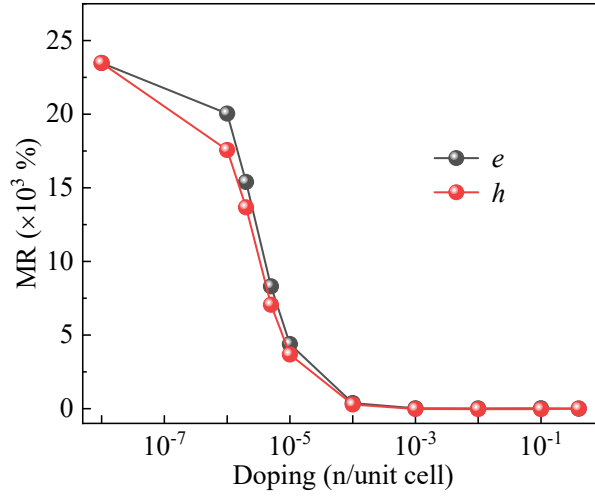


FIG. S5. Calculated MR ratio of monolayer TiCr_2N_4 under electrostatic doping.

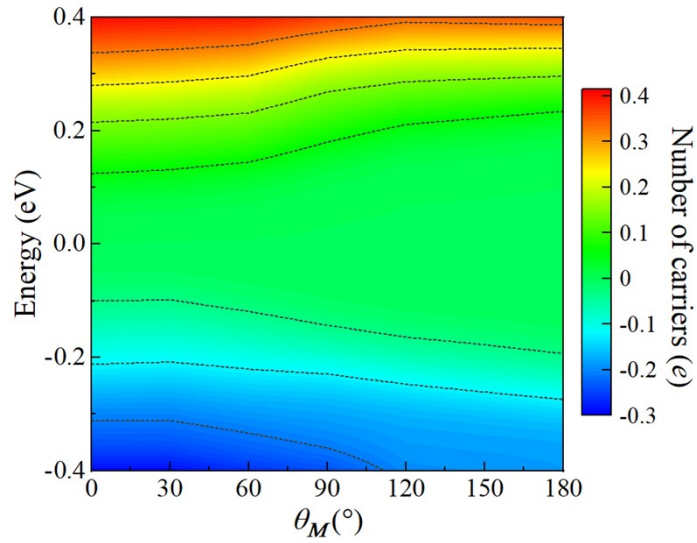


FIG. S6. Number of carriers near Fermi level under different magnetization angle between the top and bottom Cr atoms.

II. Perturbation theory analysis on magnetic anisotropy.

The spin-orbit coupling (SOC) Hamiltonian can be expressed as

$$H^{SL} = \lambda \mathbf{S} \cdot \mathbf{L} = \lambda(S_x L_x + S_y L_y + S_z L_z).$$

When the magnetization direction is characterized by the Euler angle θ and φ , one can obtain

$$H^{SL} = \lambda S(\cos \varphi \sin \theta L_x + \sin \varphi \sin \theta L_y + \cos \theta L_z).$$

The SOC induced energy the variation on total energy comes in the second-order term of the perturbation

$$E^{SL} = -\sum_{o,u} \frac{\left| \langle o | H^{SL} | u \rangle \right|^2}{\delta_{uo}}.$$

Due to the empty spin-down states, only two types of SOC need to be considered, which are $\langle o^\uparrow | H^{SL} | u^\uparrow \rangle$ and $\langle o^\uparrow | H^{SL} | u^\downarrow \rangle$. For TiCr_2N_4 monolayer, the occupied state is e_g^\uparrow . The unoccupied states are t_{2g}^\uparrow , e_g^\downarrow , and t_{2g}^\downarrow , respectively. Based on the occupancy, the variation on SOC energy is

$$\begin{aligned} E_{(\theta,\varphi)}^{SL} &= -\lambda^2 \left(\frac{\left| \langle e_g^\uparrow | \mathbf{S} \cdot \mathbf{L} | t_{2g}^\uparrow \rangle \right|^2}{\delta_1^{\uparrow\uparrow}} + \frac{\left| \langle e_g^\uparrow | \mathbf{S} \cdot \mathbf{L} | e_g^\downarrow \rangle \right|^2}{\delta_1^{\uparrow\downarrow}} + \frac{\left| \langle e_g^\uparrow | \mathbf{S} \cdot \mathbf{L} | t_{2g}^\downarrow \rangle \right|^2}{\delta_2^{\uparrow\downarrow}} \right) \\ &= -\lambda^2 \frac{1}{4} \left(\frac{\cos^2 \theta + 3}{\delta_1^{\uparrow\uparrow}} + \frac{4 \sin^2 \theta}{\delta_1^{\uparrow\downarrow}} + \frac{\sin^2 \theta + 6}{\delta_2^{\uparrow\downarrow}} \right) \\ &= -\lambda^2 \frac{1}{4} \left(-\frac{1}{\delta_1^{\uparrow\uparrow}} + \frac{4}{\delta_1^{\uparrow\downarrow}} + \frac{1}{\delta_2^{\uparrow\downarrow}} \right) \sin^2 \theta - \lambda^2 \frac{1}{4} \left(\frac{4}{\delta_1^{\uparrow\uparrow}} + \frac{6}{\delta_2^{\uparrow\downarrow}} \right) \end{aligned}$$

, which shows no dependence on the angle φ . Then, MAE can be obtained via

$$\text{MAE} = E_\theta - E_x = A \cos^2 \theta, \text{ where } A = \frac{\lambda^2}{4} \left(-\frac{1}{\delta_1^{\uparrow\uparrow}} + \frac{4}{\delta_1^{\uparrow\downarrow}} + \frac{1}{\delta_2^{\uparrow\downarrow}} \right) \text{ is treated as is a normalized}$$

parameter.

III. Band gap induced variation on MR ratio.

For semiconductors, conductivity can be calculated by $\sigma = nq\mu$, where n is the carrier concentration, q is the charge of an electron or hole, and μ is the carrier mobility, respectively. The variation on carrier concentration induced by change of band gaps is $n = n_0 e^{-E_{\text{gap}}/2k_B T}$. Then, the MR ratio can be estimated via

$$\begin{aligned}
MR &= \frac{\sigma_{\theta_M} - \sigma_{AP}}{\sigma_{AP}} \times 100\% = \frac{(n_{\theta_M} - n_{AP})q\mu}{n_{AP}q\mu} \times 100\% \\
&= \frac{n_{\theta_M} - n_{AP}}{n_{AP}} \times 100\% = \frac{e^{-E_{\theta_M}/2k_B T} - e^{-E_{AP}/2k_B T}}{e^{-E_{AP}/2k_B T}} \times 100\% \\
&= (e^{(E_{AP} - E_{\theta_M})/2k_B T} - 1) \times 100\% \\
&\approx e^{\frac{\Delta E_{gap}}{2k_B T}} \times 100\%
\end{aligned}$$

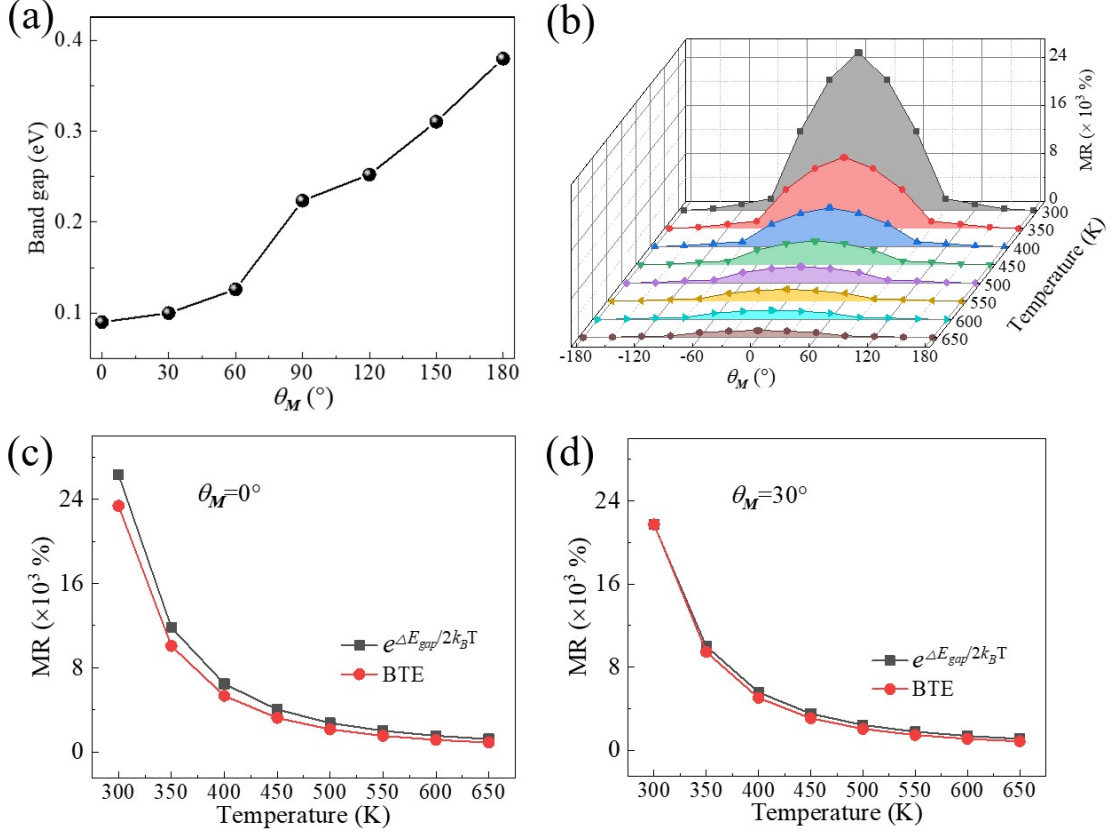


FIG. S7. (a) The value of band gaps under different θ_M and (b) evaluation of MR ratio by using band gaps of the TiCr₂N₄ monolayer. Comparison of MR ratio obtained from different methods at (c) $\theta_M = 0^\circ$ and (d) $\theta_M = 30^\circ$, respectively

IV. Projected density of states and band structures.

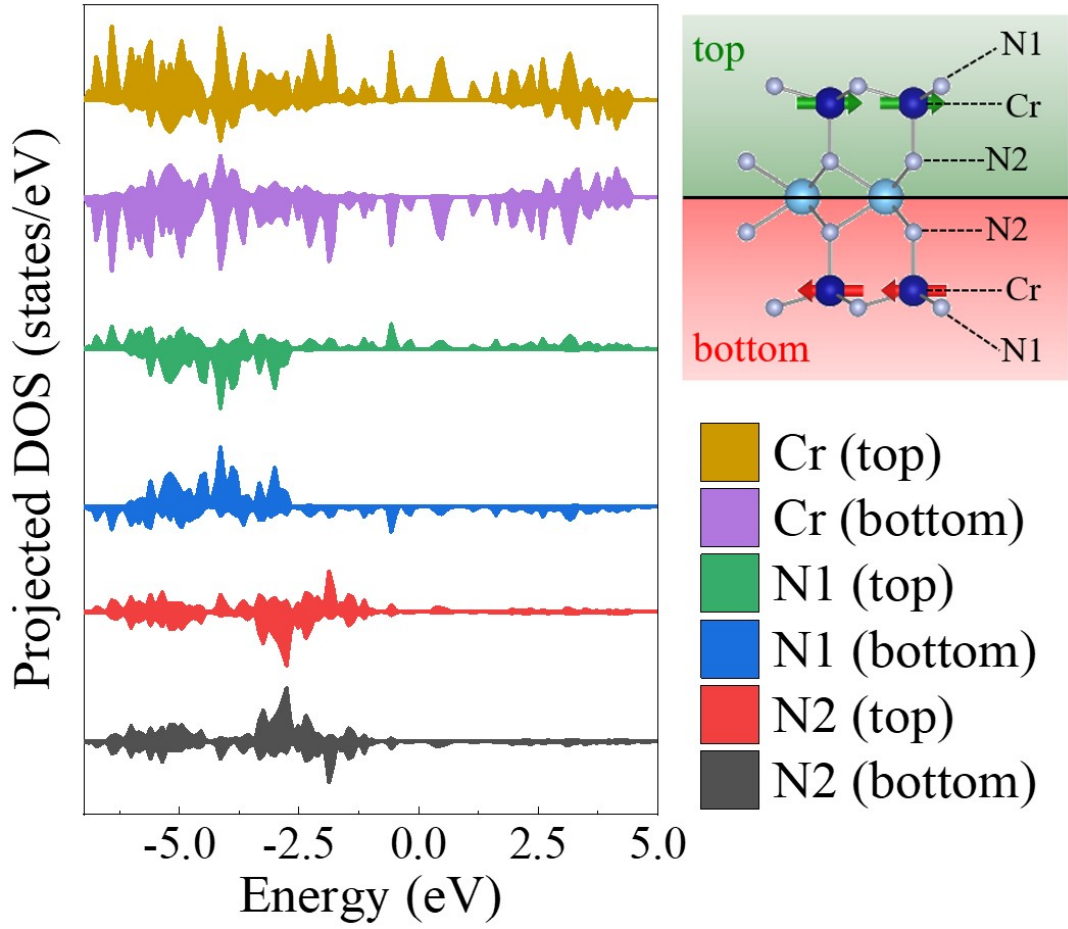


Fig. S8. Projected density of states (DOS) of TiCr_2N_4 monolayer under AP configuration.

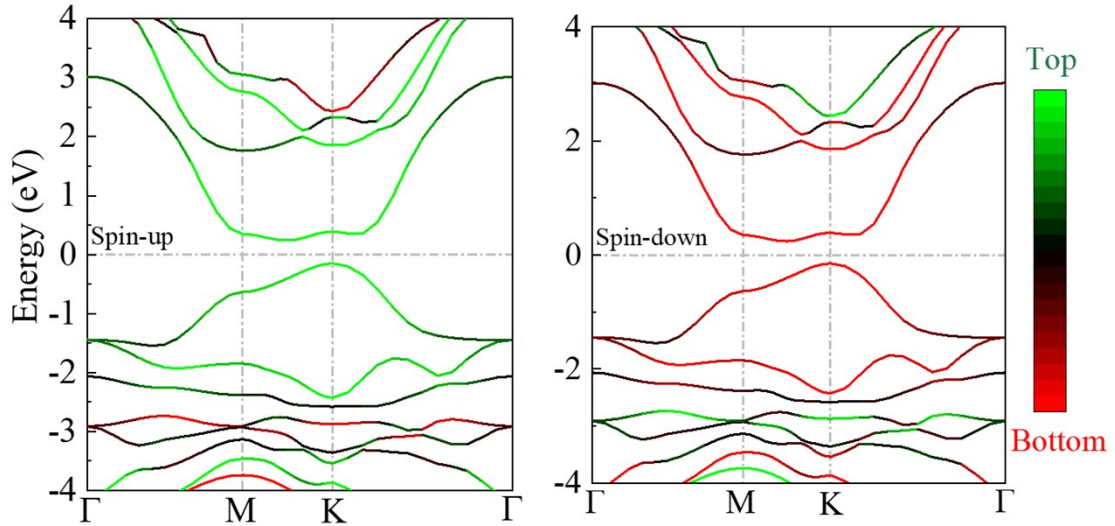


Fig. S9. Donation of the top and bottom atoms for the band structures under AP configuration.